ISSN 1541-308X, Physics of Wave Phenomena, 2015, Vol. 23, No. 1, pp. 28–34. © Allerton Press, Inc., 2015.

QUANTUM KINETICS OF SUPERLATTICES

Effect of Interminiband Tunneling on Complex Processes in a Semiconductor Superlattice

A. G. Balanov[1,2*], A. A. Koronovskii[1,3], O. I. Moskalenko[1,3***], A. O. Selskii[1,3****], and A. E. Hramov[1,3*****]**

[1] *Yuri Gagarin State Technical University of Saratov, ul. Politechnicheskaya 77, Saratov, 410054 Russia*

[2] *Loughborough University, Loughborough LE11 3TU, United Kingdom*

[3] *Saratov State University, ul. Astrakhanskaya 83, Saratov, 410012 Russia*

Received August 1, 2014

Abstract—Spectra of current oscillations caused by the transport of the electron domains induced by an applied voltage in a semiconductor superlattice with the absence and presence of the tilted magnetic field are numerically investigated with allowance for the interband tunneling.

DOI: 10.3103/S1541308X15010045

1. INTRODUCTION

Semiconductor superlattices are nanostructures that consist of alternating thin layers of semiconductors, which can be used for generating and controlling high-frequency oscillations [1]. If the period of the superlattice is smaller than the coherent length (about 6 nm) and the width of the minibands is tens of millielectronvolts (strongly coupled superlattices), the width of the bandgap between the first and second minibands can be as large as ∼200 meV. Weakly coupled superlattices are characterized by a period of more than 10 nm and small widths of minibands (<1 meV) and the bandgap (∼100 meV). In strongly coupled superlattices, electron transport is mainly determined by the motion along the first miniband while in weakly coupled superlattices the typical transport mechanism is a cascade of electron interminiband tunneling processes [2, 3].

In strongly coupled superlattices, the applied voltage gives rise to the generation of electron domains that move along the structure. Domain transport through the superlattice results in oscillations of the current through the superlattice. Earlier it was shown that the presence of a tilted magnetic field increases the amplitude and frequency of the oscillations [4, 5]. In this work, we investigate the effect of the interminiband tunneling on the oscillations of the current through the semiconductor superlattice. We expect that the results of this investigation can be used for optimizing parameters of the output signal of the semiconductor superlattice.

2. SIMULATION OF DOMAIN TRANSPORT WITH ALLOWANCE FOR INTERBAND TUNNELING

The main objective of this work is to investigate the effect of inteminiband tunneling on complex processes in a semiconductor superlattice by examining current oscillation spectra for different widths of the bandgap. To this end, various earlier proposed methods for simulation of semiconductor superlattices are used.

Processes in a semiconductor superlattice were simulated using a system of equations that includes the continuity equation

$$e\frac{\partial n}{\partial t} = \frac{\partial J}{\partial x}, \tag{1}$$

the Poisson equation

$$\frac{\partial F}{\partial x} = \frac{e}{\varepsilon_0 \varepsilon_\mathrm{r}}(n - n_\mathrm{D}), \tag{2}$$

and the expression for the current density allowing for the electron drift velocity [5, 6]

$$J = env_\mathrm{d}(F). \tag{3}$$

Here t is the time; the x coordinate corresponds to the direction perpendicular to the superlattice layers; the variables $n(x,t)$, $F(x,t)$, and $J(x,t)$ determine

*E-mail: a.balanov@lboro.ac.uk
**E-mail: alexey.koronovskii@gmail.com
***E-mail: o.i.moskalenko@gmail.com
****E-mail: feanorberserk@gmail.com
*****E-mail: hramovae@gmail.com

the concentration, the electric field strength, and the current density, respectively; ε_0 and ε_r are the absolute and the relative permittivity; n_D is the equilibrium electron concentration; v_d is the electron drift velocity calculated for the electric field strength F; and e is the electron charge.

Following [4, 7], we think the contacts of the superlattice emitter and collector to be ohmic. Then the current density J_0 through the emitter will be dictated by the contact conductance $\sigma = 3788\,\Omega^{-1}$: $J_0 = \sigma F(0)$. The electric field strength $F(0)$ can be found from the boundary conditions

$$V = U + \int_0^L F(x)\,dx, \tag{4}$$

where V is the voltage applied to the superlattice and U describes the voltage drop at the contacts [7].

When there is no tilted magnetic field, the dependence of the drift field on the electric field strength at low temperatures can be calculated analytically using the Esaki–Tsu formula [3]

$$v_d = \frac{\Delta d}{2\hbar}\frac{\omega_B\tau}{(\omega_B\tau)^2+1}, \tag{5}$$

where Δ is the width of the first miniband, d is the period of the superlattice, τ is the effective time of electron scattering, and $\omega_B = eFd/\hbar$ is the Bloch oscillation frequency. When there is a tilted magnetic field, dependences of the drift velocity on the electric field strength were calculated using the semiclassical theory [4, 8, 9]. The possibility of the tunneling between the first and second minibands was consideered using the approach described in [3]. According to this work, the drift velocity is determined with allowance for the interminiband tunneling as

$$v_{d,mod} = v_d\big[1 - T(F)\big] + T(F)\,v_{d,free}, \tag{6}$$

$$v_{d,free} = \frac{eF\tau}{2m^*}\cos^2\theta. \tag{7}$$

Here m^* is the effective mass of the electron in the semiconductor, θ is the tilting angle of the magnetic field with respect to the x axis, and $v_{d,free}$ is the electron drift velocity in the second miniband calculated in the free-electron approximation. The interminiband tunneling probability $T(F)$ is determined in accordance with [3, 10] as

$$T(F) = \exp\left(-\frac{m^* d E_g^2}{4\hbar^2|eF|\cos\theta}\right), \tag{8}$$

where E_g is the width of the bandgap between the first and second minibands. Cosines in (4) and (5) indicate the presence of the tilted magnetic field applied at an angle θ with respect to the semiconductor superlattice.

The simulation was performed with the following parameters that describe real devices and were used in experiments [2, 9]: $m^* = 0.067m_e$, where m_e is the mass of the free electron; $\Delta = 19.1$ meV; $d = 8.3$ nm, $\tau = 0.25$ ps; $n_D = 3\times10^{22}\,\mathrm{m}^{-3}$; $\varepsilon_r = 12.5$; magnetic field induction $B = 15$ T; and $\theta = 40°$.

As follows from (3), to obtain the time realizations of the current through the semiconductor superlattice we should know the dependence of the drift velocity on the electric field strength. These dependences are shown in Figs. 1(a) and 1(b) for different widths of the bandgap between the first and second minibands and configurations of the magnetic field. Different widths of the bandgap were considered in accordance with (6). When there was no tilted magnetic field, dependence (5) was taken as an unmodified drift velocity, and when there was a field, the dependence was numerically calculated according to [8].

3. RESULTS OF SIMULATION OF SEMICONDUCTOR SUPERLATTICE WITH INTERBAND TUNNELING

As follows from (8), the probability of electron tunneling from the first miniband to the second one increases with increasing electric field strength and decreasing bandgap E_g. As is evident from Figs. 1(a) and 1(b), the decrease in the tunneling probability leads to an appreciable increase in the drift velocity at a high electric field strength. This is because the drift velocity in the second miniband, where the electron moves freely, is higher than in the first miniband and thus the general drift velocity increases with increasing number of electrons in the second miniband. With the tilted magnetic field, the tunneling-related effects are less distinct because, according to (8), the cosine of the field tilting angle yields the value smaller than unity.

Examples of the time realizations obtained are shown in Figs. 1(c) and 1(d). Given the identical voltage and bandgap, the oscillations in the presence of the tilted magnetic field are usually more complex, having a pronounced peak and a few lower neighboring peaks. In the absence of the tilted magnetic field and at a low voltage, the oscillations are close to harmonic ones, but their shape changes with growing voltage, as shown in the figure. It is worth mentioning that the current oscillation frequency is also higher in the presence of the tilted magnetic field (with other parameters being equal).

Power spectra were constructed using current realizations with a duration of about 10 ns obtained with different voltages applied to the superlattice and the

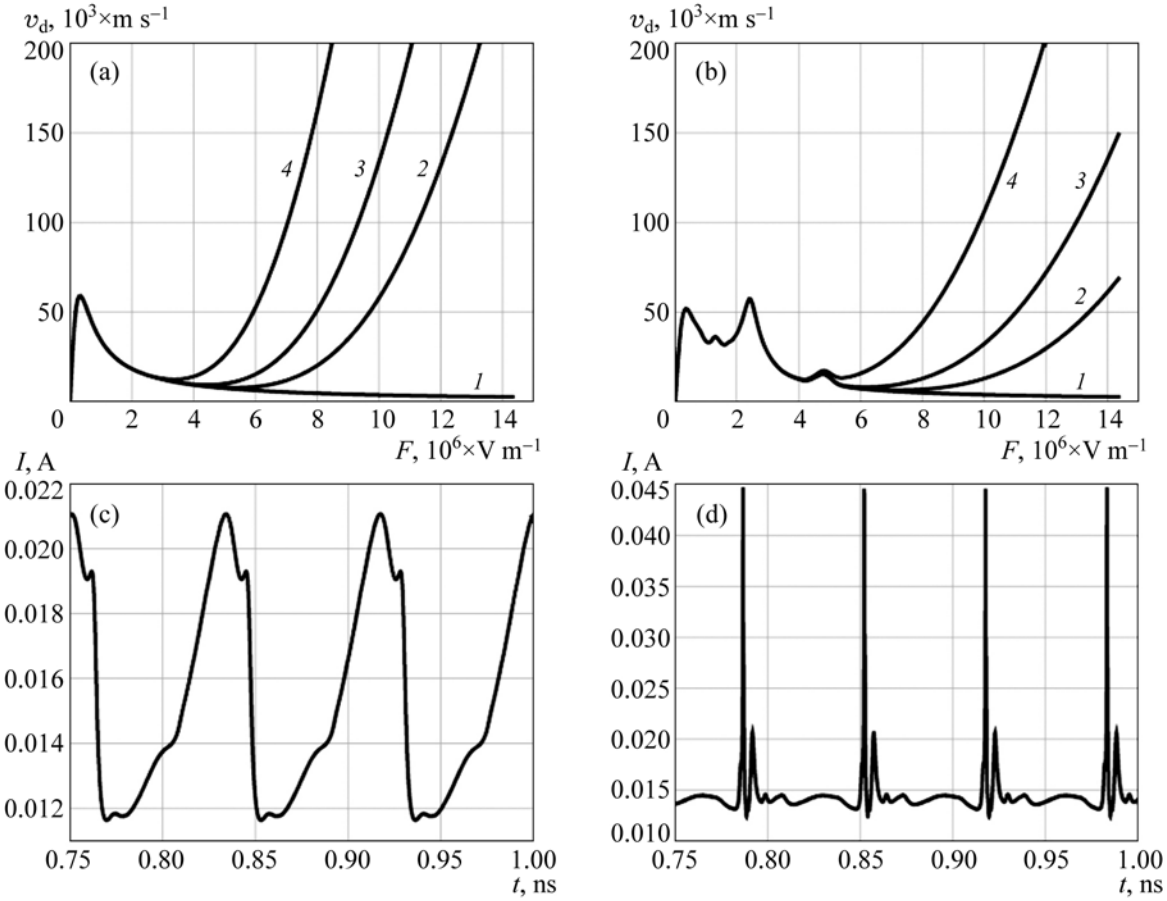

Fig. 1. (a, b) Dependences of the electron drift velocities on the electric field strength for different widths of the bandgap between the first and second energy minibands in the absence of the tilted magnetic field (a) and in the presence of the tilted magnetic field $B = 15$ T, $\theta = 40°$ (b). The bandgap are $E_g = 200$ meV (*1*), 150 meV (*2*), 130 meV (*3*), and 110 meV (*4*). (c, d) Time realizations of the current for the voltage $V = 0.8$ V and the bandgap $E_g = 150$ meV in the absence of the tilted magnetic field (c) and in the presence of the tilted magnetic field $B = 15$ T, $\theta = 40°$ (d).

bandgaps between the first and second minibands in the absence and presence of the tilted magnetic field.

Let us first examine the case with no tilted magnetic field and two voltages, $V = 0.4$ V (close to the onset of the current oscillation generation) and $V = 0.7$ V (at the developed generation). We begin with considering the effect of the interminiband electron tunneling on the oscillation power of the current through the semiconductor superlattice at $V = 0.4$ V. It follows from (4) that as the voltage applied to the superlattice increases, the electric field strength increases as well, and so, consequently, does the electron tunneling probability at the same bandgap. It is thus obvious that no interminiband tunneling effect is observed at low voltages (Figs. 2(a), 2(c), 2(e)). The power spectra under consideration are constructed for several bandgaps: $E_g = 200$ meV, when the tunneling probability is negligibly low; $E_g = 130$ meV, when tunneling rather strongly affects the electron group dynamics; and $E_g = 150$ meV, an intermediate case.

The situation appreciably changes at the voltage $V = 0.7$ V. Here the change in the width of the bandgaps between the first and second minibands produces a substantional effect on the power spectra (Figs. 2(b), 2(d), 2(f)). Both the power of the fundamental oscillation frequency and the frequency itself change: the frequency gradually decreases with increasing interminiband tunneling probability. As the tunneling probability increases, the power of the fundamental frequency first grows but then slightly diminishes. This means that the initially present electrons that tunneled to the second miniband cause an increase in the power, but the power decreases as the number of the electrons increases. The effect is due to the number of the tunneled electrons and thus to the interminiband tunneling probability rather than to a change in the width of the bandgap and is confirmed by the fact that this effect is not observed at

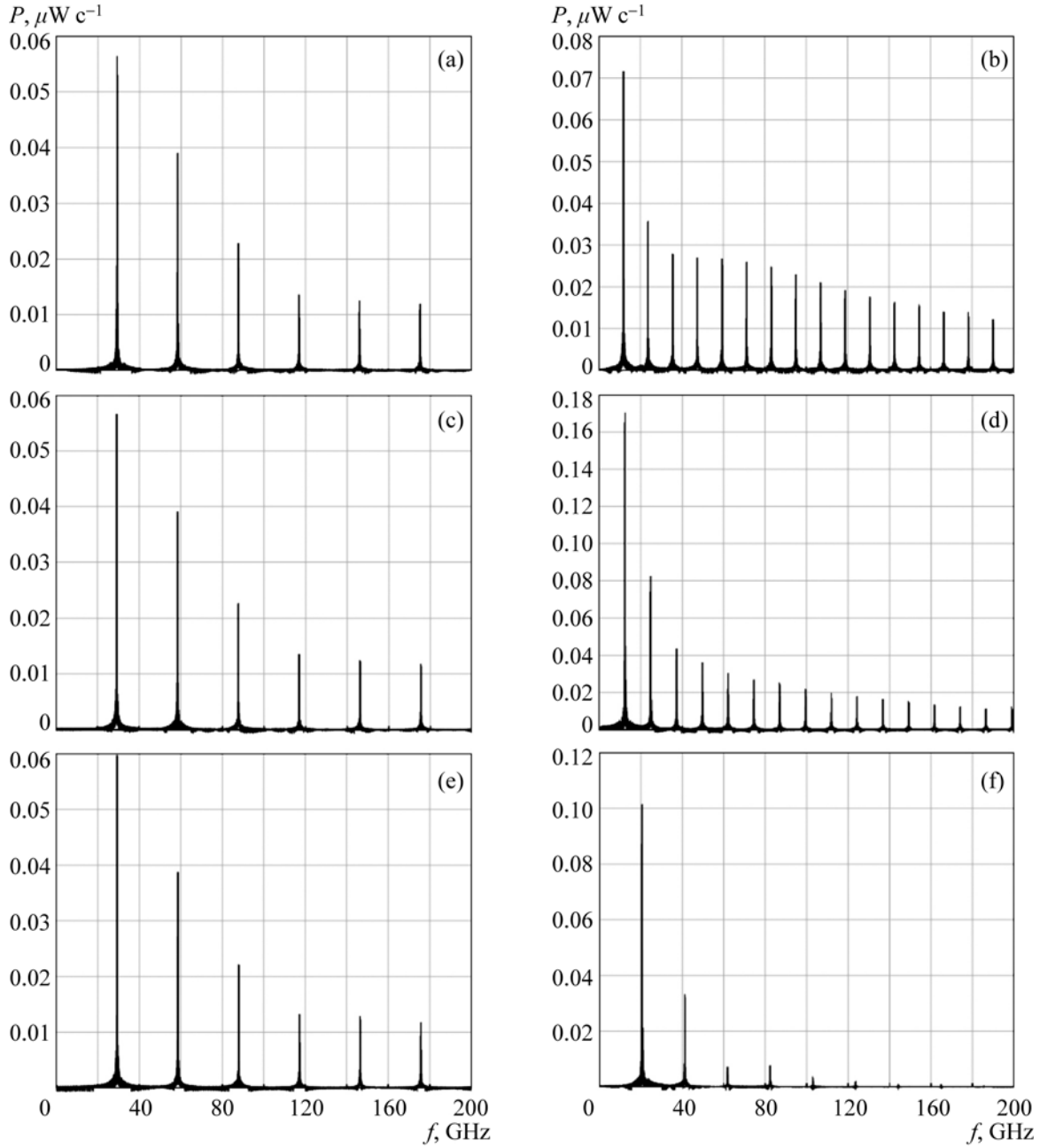

Fig. 2. Spectral power densities of current oscillation in the absence of the tilted magnetic field for different voltages and widths of the bandgap between the first and second energy minibands: (a, c, e) $V = 0.4$ V, (b, d, f) $V = 0.7$ V, (a, b) $E_g = 200$ meV, (c, d) $E_g = 150$ meV, (e, f) $E_g = 130$ meV.

$V = 0.4$ V, when the width changes at an almost constant tunneling probability (because of relatively low electric field strength), see Figs. 2(a), 2(c), and 2(e).

For any width of the bandgap between the first and second minibands the change in the voltage leads to identical results. A comparison of Figs. 2(a), 2(c), 2(e) and 2(b), 2(d), 2(f) shows that an increase in the voltage leads to a decrease in the fundamental frequency with increasing power. An exception is the case with $V = 0.7$ V and $E_g = 130$ meV, where the effects arising from the interminiband tunneling are rather strong that results in suppression of all harmonics in the spectrum except the fundamental frequency. However, the power of the fundamental frequency is higher than at $V = 0.4$ V.

Now let us examine the case where the tilted magnetic field is applied. Again, we choose two voltages $V = 0.4$ V, which is close to the threshold value (the threshold value of the voltage applied to the semiconductor superlattice is the value at which

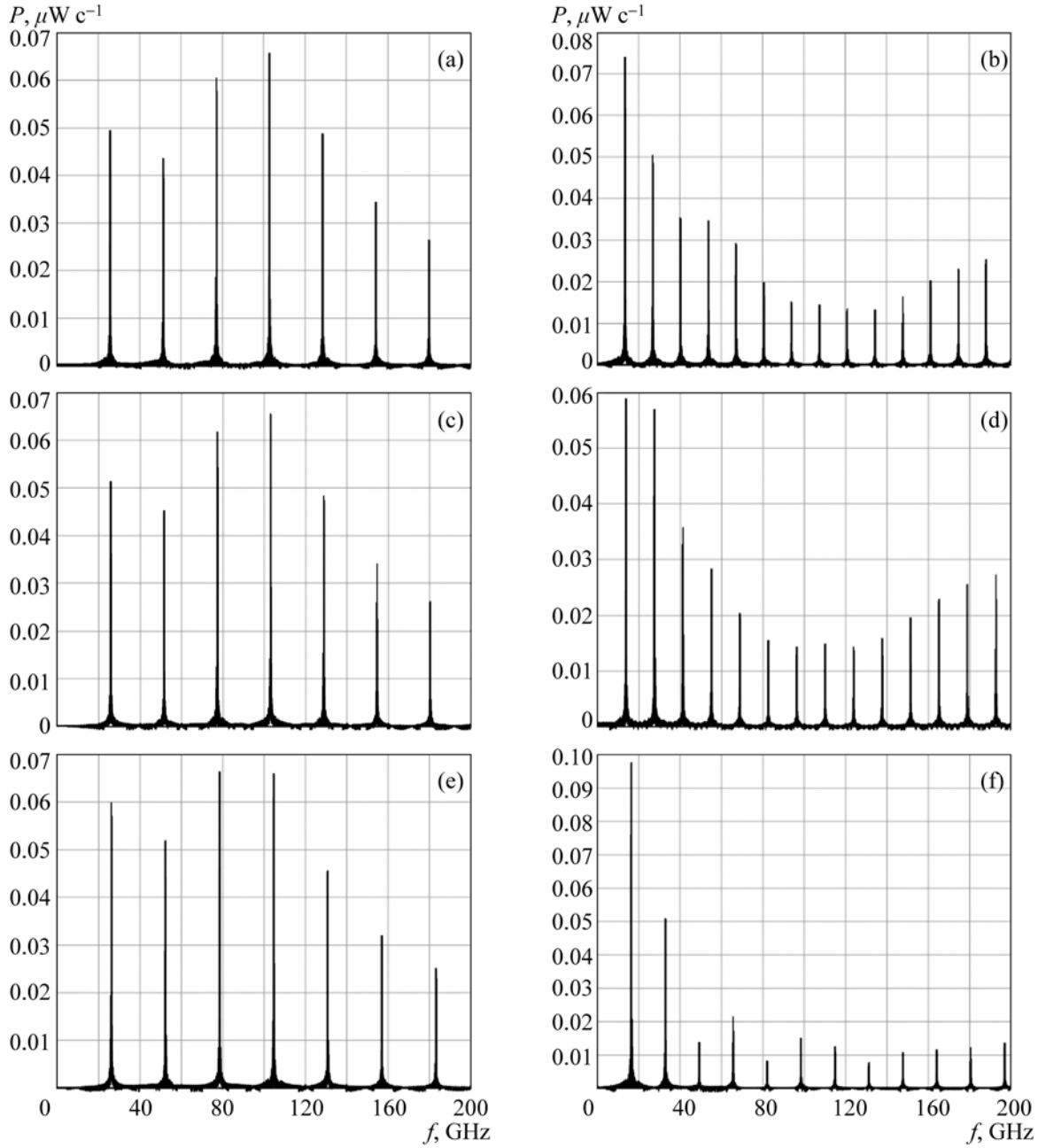

Fig. 3. Spectral power densities of current oscillation in the presence of the tilted magnetic field $B = 15$ T, $\theta = 40°$ for different voltages and widths of the bandgap between the first and second energy minibands: (a, c, e) $V = 0.6$ V, (b, d, f) $V = 0.9$ V, (a, b) $E_g = 200$ meV, (c, d) $E_g = 150$ meV, (e, f) $E_g = 130$ meV.

the generation of oscillations of the current through the superlattice begins; note that in the presence of the tilted magnetic field generation begins at high voltages [4]) and $V = 0.9$ V, when the generation is well developed. As in the case with no tilted magnetic field, at the lower voltage the electron tunneling probability is high even at a small width of the bandgap, $E_g = 130$ meV, and the effect of the interminiband tunneling is insignificant (Figs. 3(a), 3(c), and 3(e)).

A comparison of the results obtained without and with the tilted magnetic field (e.g., at $E_g = 200$ meV for definiteness), when tunneling can be ignored, reveals an interesting effect (see Figs. 2(a), 2(b) and 3(a), 3(b)). In the absence of the tilted magnetic field, the power in the spectrum decreases with increasing harmonic number while in the presence of the tilted magnetic field the observed situation is much more complicated. At a sufficiently high voltage $V = 0.9$ V

the power of harmonics is seen first to decrease and then to increase. At a low voltage $V = 0.6$ V applied to the semiconductor superlattice, the power of the fourth harmonic can be higher than the power of the fundamental frequency. This effect can be employed for increasing the generation power at higher harmonics, which is important for increasing the generation frequency of the system. Comparing the drift velocity profiles in Figs. 1(a) and 1(b) we can see that in the presence of the tilted magnetic field more peaks appear in addition to the Esaki–Tsu peak resulting from the electron scattering. These peaks correspond to the resonances of the Bloch and cyclotron frequencies and are responsible for the more complicated group dynamics observed in Figs. 1(c) and 1(d).

In the presence of the tilted magnetic field at the width of the bandgap between the first and second minibands $E_g = 200$ meV, an increase in voltage entails an increase in the power spectrum of the fundamental component, as in the case when there is no tilted magnetic field. In addition, the power ratio between the fundamental frequency and the fourth harmonic is changed. As was mentioned above, at a low voltage like $V = 0.4$ V the power of the fourth harmonic is higher than the power of the fundamental frequency, but the latter increases with voltage.

Let us return to the effects associated with the interminiband tunneling. At the voltage $V = 0.9$ V applied to the semiconductor superlattice, the probability for the electron tunneling from the first miniband to the second one is quite high. When there is no tilted magnetic field, the fundamental frequency power first increases with interminiband tunneling probability and then decreases. When there is a tilted magnetic field, the reverse is true: the fundamental frequency power first decreases and then increases (Figs. 3(b), 3(d), 3(f)). However, as was pointed out above, the interminiband tunneling probability in the presence of the tilted magnetic field is lower (see (8)). The effects arising from the interminiband tunneling depend on the tunneling probability rather than directly on the width of the bandgap, otherwise those effects could also be observed at a low voltage. In the presence of the tilted magnetic field with the bandgap decreasing, $E_g < 130$ meV, and the voltage being high, $V = 0.9$ V, the intensity of the fundamental frequency in the spectrum should decrease. Thus, it follows that as the interminiband tunneling probability increases, the power of generation at the fundamental frequency of the domain transport begins oscillations. In the context of semiconductor superlattice applications, it is of interest and current importance to investigate the above inference and find the probability for the electron tunneling from the first miniband to the second one that corresponds to the highest power at the given parameters.

4. CONCLUSIONS

The effect of the interminiband tunneling on the complex processes in a semiconductor superlattice is considered in the work. Spectral power densities of oscillations on the semiconductor superlattice are analyzed at different voltages applied to the semiconductor superlattice and widths of the bandgap between the first and second minibands in the absence and presence of the tilted magnetic field. The main result of the work is the conclusion that the power of the generation at the fundamental frequency of the domain transport begins oscillating as the interminiband tunneling probability increases that can be used for optimizing the output signal parameters of the semiconductor superlattice.

ACKNOWLEDGMENTS

The work has been supported by the Russian Scientific Foundation in the framework of study of the semiconductor superlattice in the titled magnetic field (Project 14-12-00222). A.E.H. acknowledges support from the Ministry of Education and Science of the Russian Federation in the framework of the providing researches (Project 931). A.O.S. thanks the Dynasty Foundation for Noncommercial Programs.

REFERENCES

1. L. Esaki and R. Tsu, Superlattice and Negative Differential Conductivity in Semiconductors // IBM J. Res. Develop. 14, 61 (1970).
2. N. Alexeeva, M.T. Greenaway, A.G. Balanov, O. Makarovsky, A. Patanè, M.B. Gaifullin, F. Kusmartsev, and T.M. Fromhold, "Controlling High-Frequency Collective Electron Dynamics via Single-Particle Complexity," Phys. Rev. Lett. **109**, 024102 (2012).
3. D.P.A. Hardwick, S.L. Naylor, S. Bujkiewicz, T.M. Fromhold, D. Fowler, A. Patanè, L. Eaves, A.A. Krokhin, P.B. Wilkinson, M. Henini, and F.W. Sheard, "Effect of Inter-Miniband Tunneling on Current Resonances Due to the Formation of Stochastic Conduction Networks in Superlattices," Physica E. **32**, 285 (2006).
4. A.O. Selskii, A.A. Koronovskii, A.E. Hramov, O.I. Moskalenko, K.N. Alekseev, M.T. Greenaway, F. Wang, T.M. Fromhold, A.V. Shorokhov, N.N. Khvastunov, and A.G. Balanov, "Effect of Temperature on Resonant Electron Transport Through Stochastic Conduction Channels in Superlattices," Phys. Rev. B. **84**, 235311 (2011).
5. M.T. Greenaway, A.G. Balanov, E. Schöll, and T.M. Fromhold, "Controlling and Enhancing Terahertz Collective Electron Dynamics in Superlattices by Chaos-Assisted Miniband Transport," Phys. Rev. B. **80**, 205318 (2009).
6. A. Wacker, "Semiconductor Superlattices: A Model System for Nonlinear Transport," Phys. Rep. **357**, 1 (2002).

7. A.G. Balanov, M.T. Greenaway, A.A. Koronovskii, O.I. Moskalenko, A.O. Sel'skii, T.M. Fromhold, and A.E. Khramov, "The Effect of Temperature on the Nonlinear Dynamics of Charge in a Semiconductor Superlattice in the Presence of a Magnetic Field," JETP. **114**(5), 836 (2012).
8. R. Scheuerer, E. Schomburg, K.F. Renk, A. Wacker, and E. Schöll, "Feasibility of a Semiconductor Superlattice Oscillator Based on Quenched Domains for the Generation of Submillimeter Waves," Appl. Phys. Lett. **81**, 1515 (2002).
9. T.M. Fromhold, A. Patanè, S. Bujkiewicz, P.B. Wilkinson, D. Fowler, D. Sherwood, S.P. Stapleton, A.A. Krokhin, L. Eaves, M. Henini, N.S. Sankeshwar, and F.W. Sheard, "Chaotic Electron Diffusion Through Stochastic Webs Enhances Current Flow in Superlattices," Nature. **428**, 726 (2004).
10. C. Zener, "A Theory of the Electrical Breakdown of Solid Dielectrics," Proc. R. Soc. London A. **145** (Iss. 855), 523 (1934).